# Determination of the Bond Length and Binding Energy of the Helium Dimer by Diffraction from a Transmission Grating

R. E. Grisenti, W. Schöllkopf, and J. P. Toennies
*Max-Planck-Institut für Strömungsforschung, Bunsenstraße 10, 37073 Göttingen, Germany*

G. C. Hegerfeldt, T. Köhler, and M. Stoll
*Institut für Theoretische Physik, Universität Göttingen, Bunsenstraße 9, 37073 Göttingen, Germany*
(Received 5 June 2000)

A molecular beam consisting of small helium clusters is diffracted from a 100 nm period transmission grating. The relative dimer intensities have been measured out to the 7th order and are used to determine the reduction of the effective slit width resulting from the finite size of the dimer. From a theoretical analysis of the data which also takes into account the van der Waals interaction with the grating bars, the bond length (mean internuclear distance) and the binding energy are found to be $\langle r \rangle = 52 \pm 4$ Å and $|E_b| = 1.1 + 0.3/ - 0.2$ mK.

PACS numbers: 33.15.–e, 03.75.Be, 21.45.+v, 36.40.Mr

Virtually all our current knowledge of the structure of molecules is based on either NMR, microwave, infrared, visible, or Raman spectroscopy—or on x-ray and electron scattering. Since these techniques all in one way or another disturb the system, they are not suitable for very weakly bound systems with large scattering lengths. Such apparently exotic systems have recently attracted considerable attention in connection with Bose-Einstein condensation of ultralow temperature gases [1].

An outstanding example of a fragile Boson molecule is the helium dimer $^4He_2$. Its existence was for a long time disputed because of its extremely small binding energy which is now thought to be about 1 mK ($\approx 10^{-7}$ eV). Presently, theory predicts the He-He potential to support only a single $s$ wave bound state [2]. While a first indication for its existence was reported in Ref. [3], diffraction experiments [4] very similar to those reported here provided the first conclusive evidence. From a quantitative experimental study of the bond length and binding energy of the dimer it is possible to probe the He-He potential which is of fundamental importance for understanding the remarkable superfluid properties of liquid helium.

The extremely weak He-He potential also has fascinating consequences for the $^4He_3$ molecule which is predicted to exhibit a long range Efimov type excited state [5]. Also the nature of the small mixed $^3He/^4He$ clusters [6] and the smallest bound $^3He$ cluster which is presently predicted to consist of about 30 atoms [7] as well as magic numbers in the large $^3He$ clusters [8] all are expected to depend sensitively on the exact shape of the two-body potential.

In a pioneering experiment Gentry and collaborators [9] used nanoscale sieves to measure the reduced transmission $T$ of dimers, compared to the monomers, through the small circular holes, with diameter $D$, of the sieve. They assumed a classical dumbbell model for the dimer and determined the bond length $\langle r \rangle$ from the expression $\langle r \rangle = D(1 - T)$ to be $\langle r \rangle = 62 \pm 10$ Å. Recently, two of the present authors were able to account for the breakup of the dimers at the edges of the holes in a quantum mechanical theory [10]. This theory predicts that transmission experiments provide an upper limit on $\langle r \rangle$ only.

The present experiments overcome these difficulties by measuring only the coherently scattered dimers which make up the intensity in the small angle low order peaks in the diffraction from a transmission grating. From the data, $\langle r \rangle$ is determined by a quantum mechanical theory which includes the surface potential of the grating bars and breakup effects. Then from $\langle r \rangle$ the binding energy is determined to be $|E_b| = 1.1 + 0.3/ - 0.2$ mK, which is the most precise determination to date.

The cluster beam diffraction apparatus is the same as recently described in Ref. [11]. The cryogenic $^4He$ source pressures $P_0$ and temperatures $T_0$ were varied between $(P_0, T_0) = (0.3\ \text{bar}, 4.5\ \text{K})$ and $(65\ \text{bar}, 65\ \text{K})$ to produce beams with an optimum fraction of dimers and with a negligible number of clusters larger than $^4He_3$. The beam is highly collimated by 5 mm high 20 $\mu$m (150 mm from the source) and 10 $\mu$m (1000 mm from the source) slits and then is diffracted from a $d = 100$ nm period ($SiN_x$) transmission grating [12]. The depth and wedge angle of the grating bars (see Fig. 1) were determined from transmission measurements [11] to be $t = 70$ nm and $\beta = 13°$, respectively.

Figure 2 shows the measured diffraction patterns at 8 different source temperatures $T_0$ between 4.5 and 65 K. The $^4He^+$ ion signal, which spans more than 4 orders of magnitude and has a maximum forward intensity of about $3 \times 10^5$ counts/sec at $T_0 = 65$ K, is plotted on a logarithmic scale versus the deflection angle $\vartheta$. The signal was detected with a mass spectrometer set at the $^4He^+$ ion mass because of the much higher probability for fragmentation to produce $^4He^+$ (95%) than $^4He_2^+$ (5%) from the $^4He_2$ molecule [13]. The equally spaced, most intense diffraction peaks in each diffraction pattern are due to atoms, while all the other peaks are due to clusters $^4He_N$. Since all clusters have the same velocity $v$ as the atoms

 0031-9007/00/85(11)/2284(4)$15.00 

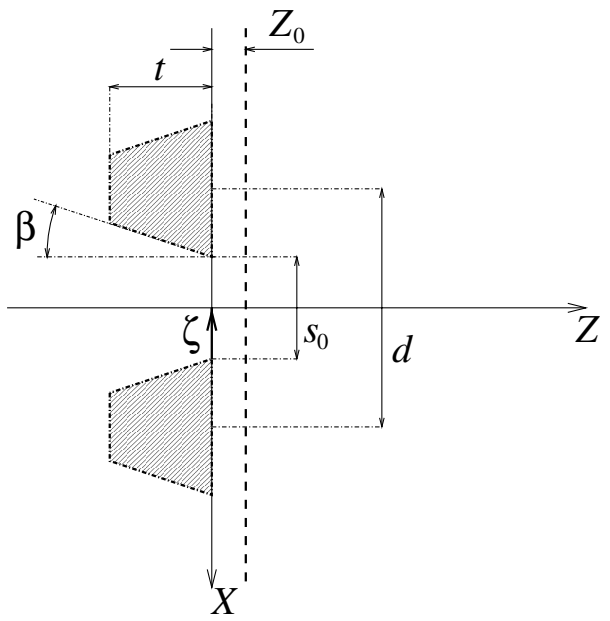


FIG. 1. Cross section of a grating slit with two bars showing their geometry and the important coordinates.

[14] their de Broglie wavelengths $\lambda$ and hence their $n$th order diffraction angles $\vartheta_n$ are inversely proportional to their mass since $\sin\vartheta_n = n\lambda/d = nh/Nmvd$. The peaks marked by an asterisk which appear halfway between the atom peaks are due to dimers. Only the odd order dimer peaks are visible, since the others coincide with the intense atom peaks. Similarly, the first order trimer peaks appear at one-third of the monomer diffraction peaks.

The relative diffraction intensities have been determined from Fig. 2 by fitting each peak with a Gaussian profile and evaluating the peak areas, thereby accounting for the different widths of the peaks due to the small $\Delta v/v \leq 2\%$ velocity spread [11].

To determine the helium dimer bond length it is necessary to derive an expression for the diffraction intensities $I_n$ of the measured dimer diffraction peaks in Fig. 2. The incident dimer wave function, which is a product of a center of mass plane wave $e^{iKZ}$ and the bound state wave function $\phi_b(\mathbf{r})$, evolves by the scattering into the scattering wave function $\psi(X, Z, \mathbf{r})$, where $\mathbf{r} = (x, y, z)$ are the relative coordinates of the dimer and $(X, Z)$ the center of mass coordinates normal to the height of the bars (see Fig. 1). The scattering wave function $\psi$ is a solution of the two-particle Schrödinger equation

$$\left[ -\frac{\hbar^2}{2M}\left(\frac{\partial^2}{\partial X^2} + \frac{\partial^2}{\partial Z^2}\right) + V_{\rm gr}(X, Z, \mathbf{r}) - \frac{\hbar^2}{2\mu}\Delta_{\mathbf{r}} + V(r)\right]\psi = \left(\frac{\hbar^2 K^2}{2M} + E_b\right)\psi , \quad (1)$$

where $M$ is the dimer mass, $\mu$ its reduced mass, $V(r)$ the He-He potential, and $V_{\rm gr}(X, Z, \mathbf{r})$ the interaction

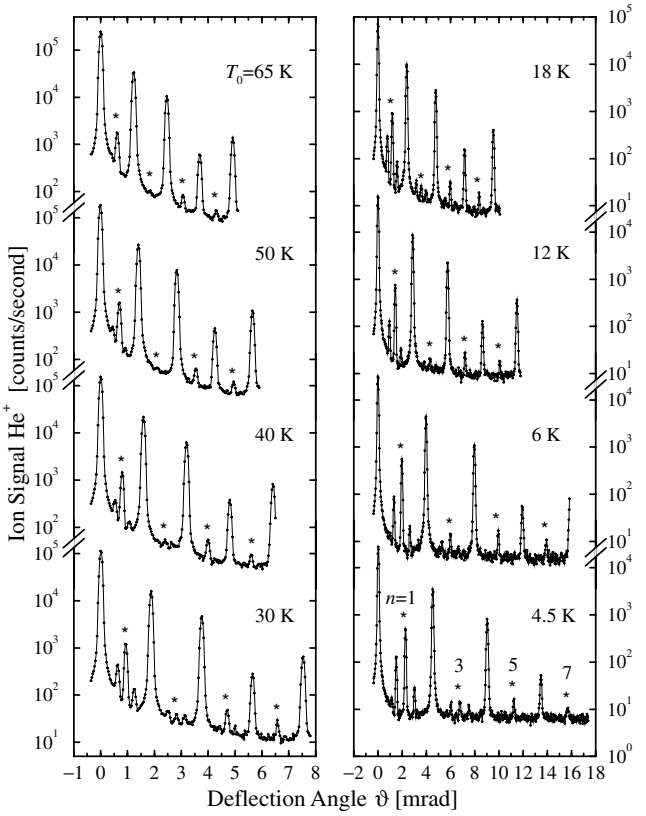


FIG. 2. Diffraction patterns of $^4$He cluster beams diffracted from a 100 nm period transmission diffraction grating with different nozzle temperatures. The odd order dimer diffraction peaks are marked by an asterisk.

of the dimer constituents with the grating [10]. Only the center of mass part of $\psi$ in the elastic channel, $\psi_{\rm el}(X, Z) \equiv \int d\mathbf{r}\,\phi_b^*(\mathbf{r})\psi(X, Z, \mathbf{r})$, is needed. For large $R = \sqrt{X^2 + Z^2}$ it becomes

$$\psi_{\rm el}(X, Z) \underset{R\to\infty}{\longrightarrow} f_{\rm el}(\vartheta)\frac{e^{i(KR-\pi/4)}}{\sqrt{R}} , \quad (2)$$

where $f_{\rm el}(\vartheta)$ is the elastic scattering amplitude. Thus, the intensity is given by $I(\vartheta) = |f_{\rm el}(\vartheta)|^2$.

Multiplying Eq. (1) from the left by $\phi_b^*(\mathbf{r})$ and integrating over $\mathbf{r}$ yields

$$\left(\frac{\partial^2}{\partial X^2} + \frac{\partial^2}{\partial Z^2} + K^2\right)\psi_{\rm el}(X, Z) = \rho(X, Z) , \quad (3)$$

where $\rho(X, Z) \equiv \frac{2M}{\hbar^2}\int d\mathbf{r}\,\phi_b^*(\mathbf{r})V_{\rm gr}(X, Z, \mathbf{r})\psi(X, Z, \mathbf{r})$. For $Z \geq Z_0$ chosen farther behind the downstream boundary of the grating than the spatial extent of the dimer (see Fig. 1), $\rho$ is negligible. Thus, Eq. (3) is homogeneous there and Huygens' principle [10] yields

$$f_{\rm el}(\vartheta) = \frac{\cos\vartheta}{\sqrt{\lambda}} e^{-iKZ_0\cos\vartheta}\int dX e^{-iKX\sin\vartheta}\psi_{\rm el}(X, Z_0) . \quad (4)$$

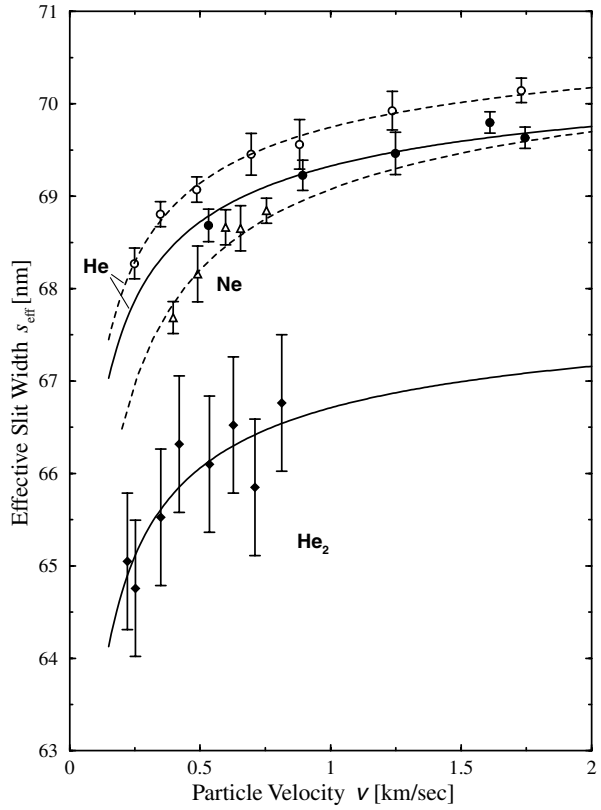


FIG. 3. Effective slit widths of He, Ne, and $^4He_2$ plotted as a function of the beam velocity. Data points indicate fits of $I_n/I_1$ determined from Eq. (5) to experimental intensity ratios obtained with the same grating in the present work (filled symbols) and previously in Ref. [15] (open symbols). The curves through the atomic effective slit widths of He and Ne are calculated as in Ref. [15]. The solid line through the effective slit widths of $^4He_2$ is a best fit curve of Eq. (7) for the $^4He_2$ bond length $\langle r \rangle$.

This is formally analogous to the diffraction of point particles [15] where the scattering amplitude is determined by a transmission function whose counterpart here is $\psi_{\mathrm{el}}(X, Z_0)$. Similarly as in Ref. [15], Eq. (4) can be used to show that the $n$th order diffraction peak intensity is of the general form

$$I_n \propto e^{-(2\pi n\sigma/d)^2}\left[\frac{\sin^2(n\pi s_{\mathrm{eff}}/d) + \sinh^2(n\pi\delta/d)}{(n\pi)^2}\right]. \tag{5}$$

Equation (5) contains a Kirchhoff slit function, where the effective slit width $s_{\mathrm{eff}}$ contains the geometrical slit width $s_0$ and corrections from the surface potential and dimer size [10,15]. These corrections enter Eq. (5) linearly while $\delta$, which suppresses the zeros of the Kirchhoff term, enters quadratically. Physically, $\delta$ reflects the diffuseness of the bar-to-slit transition due to the surface potential. The exponential damping term in Eq. (5) can be attributed in part to the breakup of dimers [10] but depends also on the van der Waals interaction of the dimer with the grating bars and on their random imperfections [11,15].

To determine $s_{\mathrm{eff}}$ Eq. (5) was used to fit the diffraction data. Figure 3 shows $s_{\mathrm{eff}}$ for $^4He_2$ and He from the present data at various velocities (filled symbols), compared with previous results for He and Ne for the same grating (open symbols). The parameters $\sigma$ and $\delta$ are of the order of 2.5 and 3 nm, respectively, for both helium atoms and dimers, and they exhibit the expected slow increase with decreasing velocity [15]. Because of lower intensities the statistical error of $s_{\mathrm{eff}}$ indicated in Fig. 3 is larger for the dimers than for the atoms. For $^4He_2$ the values for $s_{\mathrm{eff}}$ are significantly smaller, by about 2.5 nm, than those for either He and Ne. Since Ne has about the polarizability of $^4He_2$, namely twice that of He, the difference must be a size effect. According to Ref. [10] the difference is predicted to be about half the bond length.

The present data for He give a geometrical slit width $s_0 = 70.8 \pm 0.3$ nm which differs by 0.4 nm from the previously reported value of $s_0 = 71.2 \pm 0.1$ nm [15] for the same grating. This small decrease may be attributed to a monolayer of residual gas. Similar small decreases in slit width have been observed in the past.

The helium dimer bond length $\langle r \rangle$ will now be determined from the effective dimer slit widths and the single-slit transmission function, $\tau(\zeta)$, for a *single* incoming helium atom [15], where $\zeta = s_0/2 - X$ (see Fig. 1). Proceeding and incorporating the surface potential as indicated in Ref. [10] yields

$$s_{\mathrm{eff}} = 2\,\mathrm{Re}\int d\mathbf{r}|\phi_b(\mathbf{r})|^2 \times \int_0^{s_0/2} d\zeta\,\tau\left(\zeta + \frac{|x|}{2}\right)\tau\left(\zeta - \frac{|x|}{2}\right). \tag{6}$$

It is important to note that in the following the precise form of $\phi_b$ will not be needed while the atomic transmission function $\tau(\zeta)$ can be calculated in terms of the geometrical slit width $s_0$ and the van der Waals surface potential

TABLE I. Comparison of the bond lengths ($\langle r \rangle$), binding energies ($E_b$), and $s$ wave scattering lengths ($a_0$) obtained in the present work with recent theoretical predictions [2,17].

| Work | $\langle r \rangle$ [Å] | $\lvert E_b \rvert$ [mK] | $a_0$ [Å] |
|---|---|---|---|
| Present | $52 \pm 4$ | $1.1 + 0.3/-0.2$ | $104 + 8/-18$ |
| TTY [2] | 51 | 1.32 | 99.5 |
| HFD-B3-FCI1 [17] | ... | 1.59 | 91.0 |
| HFD-B3-FCI1 with retardation [17] | ... | $1.5 \pm 0.1$ | $94 \pm 2$ |

$-C_3/l^3$, where $l$ is the distance from the surface [15]. A change of variable $\zeta \to \zeta - |x|/2$ in Eq. (6) gives for the inner integral $\int_0^{(s_0-|x|)/2} d\zeta\tau(\zeta)\tau(\zeta + |x|)$. In the middle of the slits ($\zeta \approx s_0/2$ in Fig. 1) one has $\tau(\zeta) = 1$ [15], and since $|x|$ is small compared to the slit width the inner integral becomes

$$\int_0^{(s_0-|x|)/2} d\zeta\tau(\zeta)\tau(\zeta + |x|) = \int_0^{s_0/2} d\zeta\tau(\zeta) \times \tau(\zeta + |x|) - \frac{|x|}{2}.$$

The spherical symmetry of $\phi_b$ implies $\langle|x|\rangle \equiv \int d\mathbf{r}|x||\phi_b(\mathbf{r})|^2 = \langle r\rangle/2$. A Taylor expansion around $\zeta + \langle|x|\rangle$ gives after an elementary calculation

$$s_{\text{eff}} = \left[2\text{Re}\int_0^{s_0/2} d\zeta\tau(\zeta)\tau(\zeta + \langle r\rangle/2)\right] - \frac{\langle r\rangle}{2}, \quad (7)$$

where higher order terms can be shown to be negligible. The first term on the right-hand side of Eq. (7) accounts for the reduction of $s_0$ by the van der Waals interaction of each atomic constituent with the grating bars. The bond length $\langle r\rangle$ is determined from Eq. (7) by calculating $\tau(\zeta)$ with the measured $s_0$ and the $C_3$ value for He from Ref. [15]. The solid curve through the experimentally determined effective slit widths of $^4He_2$ in Fig. 3 represents a least-squares fit which yields $\langle r\rangle = 52 \pm 4$ Å.

For potentials with a nearly resonant $s$ wave bound state, as in the case of the helium dimer interaction, the binding energy is given by the approximate expression [16] $|E_b| = \hbar^2/4m\langle r\rangle^2$ where $m$ is the $^4$He mass. In the case of the Tang-Toennies-Yiu (TTY) potential [2], there is an upward correction of 12%. The $s$ wave scattering length is $a_0 = 2\langle r\rangle$ [16] with a similar downward uncertainty. Table I shows a comparison of the present results with theoretical predictions of the perturbation theory TTY potential [2] and of the HFD-B3-FCI1 potential, regarded as the most accurate [17], with and without retardation corrections.

Size determination by transmission gratings should be applicable also to other extended diatomic or polyatomic molecules. An ideal candidate is the three-body helium van der Waals molecule. Theory predicts the existence of a ground state $^4He_3$ and a single excited state $^4He_3^*$ in the helium trimer where the latter is believed to be an Efimov state [5]. While the ground state is expected to be extended on the scale of 1 nm the Efimov state should be even larger than the helium dimer. Thus the extent to which $^4He_3^*$ is present in a helium-trimer beam could be determined from the diffraction intensities due to its enormous spatial extent. This could provide evidence for an Efimov state [18].

We are greatly indebted to Tim Savas and Henry I. Smith, MIT, for providing the nanoscale transmission grating to us. Further, we thank W. Sandhas, L. W. Bruch, M. Lewerenz, and J. R. Manson for inspiring discussions.

[1] M. Arndt, M. Ben Dahan, D. Guéry-Odelin, M. W. Reynolds, and J. Dalibard, Phys. Rev. Lett. **79**, 625 (1997).
[2] K. T. Tang, J. P. Toennies, and C. L. Yiu, Phys. Rev. Lett. **74**, 1546 (1995).
[3] F. Luo, G. C. McBane, G. Kim, C. F. Giese, and W. R. Gentry, J. Chem. Phys. **98**, 3564 (1993).
[4] W. Schöllkopf and J. P. Toennies, Science **266**, 1345 (1994).
[5] V. N. Efimov, Comments Nucl. Part. Phys. **19**, 2371 (1990).
[6] B. D. Esry, C. D. Lin, and C. H. Greene, Phys. Rev. A **54**, 394 (1996); D. Bessanini, M. Zavaglia, M. Mella, and G. Morosi, J. Chem. Phys. **112**, 717 (2000); W. Schöllkopf, J. P. Toennies, and M. Lewerenz (to be published).
[7] M. Barranco, J. Navarro, and A. Poves, Phys. Rev. Lett. **78**, 4729 (1997); R. Guardiola and J. Navarro, Phys. Rev. Lett. **84**, 1144 (2000).
[8] C. Yannouleas and U. Landman, Phys. Rev. B **54**, 7690 (1996).
[9] F. Luo, C. F. Giese, and W. R. Gentry, J. Chem. Phys. **104**, 1151 (1996).
[10] G. C. Hegerfeldt and T. Köhler, Phys. Rev. A **61**, 023606 (2000).
[11] R. E. Grisenti, W. Schöllkopf, J. P. Toennies, J. R. Manson, T. A. Savas, and H. I. Smith, Phys. Rev. A **61**, 033608 (2000).
[12] T. A. Savas, S. N. Shah, M. L. Schattenburg, J. M. Carter, and H. I. Smith, J. Vac. Sci. Technol. B **13**, 2732 (1995).
[13] W. Schöllkopf and J. P. Toennies, J. Chem. Phys. **104**, 1155 (1996).
[14] D. R. Miller, in *Atomic and Molecular Beam Methods,* edited by G. Scoles (Oxford University Press, New York, 1988).
[15] R. E. Grisenti, W. Schöllkopf, J. P. Toennies, G. C. Hegerfeldt, and T. Köhler, Phys. Rev. Lett. **83**, 1755 (1999).
[16] J. M. Blatt and V. F. Weisskopf, *Theoretical Nuclear Physics* (Springer, New York, 1979), pp. 48–65; J. Lekner, Mol. Phys. **23**, 619 (1972).
[17] A. R. Janzen and R. A. Aziz, J. Chem. Phys. **103**, 9626 (1995).
[18] An alternative approach is based on the excitation of ground-state helium trimers during the diffraction from a transmission grating [see G. C. Hegerfeldt and T. Köhler, Phys. Rev. Lett. **84**, 3215 (2000)].